

Prediction and Control of the Bi-stable Functionally Graded Composites by Temperature Gradient Field

Zheng ZHANG*, Gangfei YE, Huaping WU, Dandi CHEN, Guozhong CHAI

Key Laboratory of E&M (Zhejiang University of Technology), Ministry of Education & Zhejiang Province, 18, Chaowang Road, Hangzhou, P.R. China

crossref <http://dx.doi.org/10.5755/j01.ms.21.4.9566>

Received 23 January 2015; accepted 19 June 2015

The bi-stable cylindrical composites, which are composed of the fiber-through-thickness variation functionally graded material (FGM) subjected to a temperature gradient field, studied in the paper. The advantages of both of the FGMs' adaptability for the temperature field variation and the bi-stability of the un-symmetric and anti-symmetric orthogonal lay-ups are combined, the presented bi-stable structure has a potential application in many fields. The thermal-induced bi-stable FGM un-symmetric and anti-symmetric orthogonal shell is studied by the finite element analysis. The different FGM lay-ups are simulated successfully by the commercial finite element software ABAQUS and its subroutines. The curved shapes, the temperature-load history and stress distributions are also given to understand this bi-stable phenomenon.

Keywords: through-thickness functionally graded material, laminated shell, bi-stable, temperature gradient field.

1. INTRODUCTION

As one of the applications of the polymer-based composite materials [1–2], bi-stable structures have both extended and roll-up stable configurations, which is suitable for morphing structures, such as airfoil section for the aerodynamic control [3], telescopic camera mount for the inspection of nuclear power stations [4–5], and other specialized potential application areas [6–13]. The bi-stable structure can change from one stable state to another stable condition by external work, piezoelectric patches or shape memory alloy actuators. Analytical model [10, 14–16] and numerical model [3, 15, 17] for the anti-symmetric laminates and un-symmetric laminates have been presented in these articles. Most of the analytical model to predict the bi-stable composites is based on the principle of minimum total potential energy, and multiple local minimum values can be obtained when the total potential energy of the structure is minimized. Each local minimum value for the total potential energy corresponds to a stable shape. It is suited to using the analytical method for simple kind bi-stable plates and shells. However, for complex structures and complicated environments, it is necessary to use powerful nonlinear finite element analysis software as the computational tools in order to predict and determine the bi-stability characteristics of the composite structures.

It's known that the environment variation, such as temperature and moisture etc., has a great influence on this kind of structures [17–19]. When the bi-stable structures subjected to a temperature gradient field, such as during the curing process or some particular application fields, the composite plate is heated up and subsequently cooled-down to room temperature, the corresponding shape

change happens. When the composite structures are affected by proper temperature gradient field, then it is possible to snap to another stable configuration. The structures under a through-thickness temperature variation can produce thermal deformations composed of in-plane expansion and out of the plane bending.

Functionally graded materials (FGMs) [20–22] possess excellently mechanical properties and environmental resistance. By varying the fiber volume fraction of the glass fiber polypropylene (Glass/PP) functionally graded material within a symmetric laminated shell to create a FGM laminated shell, the material properties of this kind FGM shell continuous changes with the material components along the thickness direction.

In this study, general equations of the bi-stable FGM composites subjected to thermal load were explained. Mechanical properties of functionally graded materials that spatial gradient of fiber content through the thickness of the structures have been investigated. Finite element analysis method considering thermally induced bi-stable structures was discussed using ABAQUS software and its subroutines. The bi-stability of two different un-symmetric and anti-symmetric orthogonal FGM shell examples was simulated and discussed. The presented work will be helpful for the designers to simulate the bi-stable FGM shell structures correctly, predict its mechanical properties easily and then control the bi-stable configurations properly.

2. BI-STABLE FGM SHELL MODEL

For fiber-reinforced materials, the lamina engineering constants including the elastic modulus and Poisson's ratio can be expressed in terms of the elastic modulus, Poisson's ratios, and volume fractions of the constituents [23].

$$E_{11} = E_f V_f + E_m V_m ; \quad (1)$$

* Corresponding author. Tel.: +86-571-88320244.
E-mail address: zhangme@zjut.edu.cn (Z. Zhang)

$$E_{22} = \frac{E_f E_m}{E_f V_m + E_m V_f}; \quad (2)$$

$$\mu_{12} = \mu_f V_f + \mu_m V_m; \quad (3)$$

$$G_{12} = \frac{G_f G_m}{G_f V_m + G_m V_f}; \quad (4)$$

$$G_f = \frac{E_f}{2(1 + \mu_f)}, \quad G_m = \frac{E_m}{2(1 + \mu_m)}, \quad (5)$$

where subscript f is for the fibers, m for the matrix. E is the elastic modulus, G the shear modulus, μ the Poisson's ratio, E_{11} is the longitudinal modulus, E_{22} is the transverse modulus, μ_{12} the primary Poisson's ratio, and G_{12} is the shear modulus. V is the volume fraction which has the relationship as below:

$$V_f + V_m = 1. \quad (6)$$

The macro mechanical properties of unidirectional composites including thermal expansion coefficients can be determined [24–26],

$$\alpha_{11} = \frac{\alpha_f E_f V_f + \alpha_m E_m V_m}{E_f V_f + E_m V_m}; \quad (7)$$

$$\alpha_{22} = \alpha_f V_f + \alpha_m V_m, \quad (8)$$

where α_{11} and α_{22} are the coefficients of linear thermal expansion (CLTE) along the fibers and across the fibers, respectively.

For functionally graded shells, the material properties P^{fgm} are also assumed to vary through the thickness of the shell as a function of the volume fraction and properties of the constituent materials. These properties can be expressed as [21–22]:

$$P^{fgm}(z) = \sum_{j=1}^k P_j V_j(z), \quad (9)$$

where P_j and V_j are the material property and volume fraction, respectively, of the constituent material j . The volume fraction of all of the constituent materials should add up to one [27]:

$$\sum_{j=1}^k V_j = 1. \quad (10)$$

From Eq. 1–Eq. 10, the expression of the material properties of the FGM shell along thickness direction z can be expressed as

$$E_{11}^{fgm}(z) = E_f V_f(z) + E_m V_m(z), \quad (11)$$

$$\mu_{12}^{fgm}(z) = \mu_f V_f(z) + \mu_m V_m(z), \quad (12)$$

$$E_{22}^{fgm}(z) = \frac{E_f E_m}{E_f V_m(z) + E_m V_f(z)}, \quad (13)$$

$$G_{12}^{fgm}(z) = \frac{E_f E_m}{2[E_f(1 + \mu_m)V_m(z) + E_m(1 + \mu_f)V_f(z)]} \quad (14)$$

$$\alpha_{11}^{fgm}(z) = \frac{\alpha_f E_f V_f(z) + \alpha_m E_m V_m(z)}{E_f V_f(z) + E_m V_m(z)}, \quad (15)$$

$$\alpha_{22}^{fgm}(z) = \alpha_f V_f(z) + \alpha_m V_m(z). \quad (16)$$

The glass-fiber-material reinforced polypropylene [28–29] is researched in the presented work. The glass fiber (GF) content in the composite continuously varies through the thickness from 10 % to 30 % by volume or from 30 % to 10 %. The bi-stable laminates are composed of the anti-symmetric or un-symmetric through-thickness Glass/PP FGM composite.

Bi-stable shapes can be obtained by using laminated structures subjected to temperature gradient field. Considering the geometric nonlinear behaviour, the thermally induced strains-displacements relationship can be written as

$$\begin{Bmatrix} \varepsilon_x \\ \varepsilon_y \\ \varepsilon_{xy} \end{Bmatrix} = \begin{Bmatrix} \varepsilon_x^0 - z \frac{\partial^2 w^0}{\partial x^2} - \alpha_x \Delta T \\ \varepsilon_y^0 - z \frac{\partial^2 w^0}{\partial y^2} - \alpha_y \Delta T \\ \varepsilon_{xy}^0 - z \frac{\partial^2 w^0}{\partial x \partial y} - \alpha_{xy} \Delta T \end{Bmatrix},$$

$$= \begin{Bmatrix} \frac{\partial u^0}{\partial x} + \frac{1}{2} \left(\frac{\partial w^0}{\partial x} \right)^2 - z \frac{\partial^2 w^0}{\partial x^2} - \alpha_x \Delta T \\ \frac{\partial v^0}{\partial y} + \frac{1}{2} \left(\frac{\partial w^0}{\partial y} \right)^2 - z \frac{\partial^2 w^0}{\partial y^2} - \alpha_y \Delta T \\ \frac{1}{2} \left(\frac{\partial u^0}{\partial y} + \frac{\partial v^0}{\partial x} + \frac{\partial w^0}{\partial x} \frac{\partial w^0}{\partial y} \right) - z \frac{\partial^2 w^0}{\partial x \partial y} - \alpha_{xy} \Delta T \end{Bmatrix} \quad (17)$$

where superscript 0 refers to the reference middle plane of the laminate. u , v , w are the displacement components in the x -, y -, z - directions, respectively.

The total potential energy (II) of a composites structure in plane-stress subjected to thermal loads can be expressed as

$$II = \int_V \left(\frac{1}{2} \overline{Q}_{ij} \varepsilon_i \varepsilon_j - \overline{Q}_{ij} \alpha_j \varepsilon_i \Delta T \right) dV \quad (i, j=1,2,6), \quad (18)$$

where V is the structural volume, ΔT is the gradient of the thermal loads. When the total potential energy of the structure is minimized, two or multiple local minimum values can be obtained.

In the theoretical framework of the classical laminated plates theory [23, 30–31]. The stress-strain relationship accounted for thermally-induced deformations in laminate coordinates for the k th layer is

$$\begin{Bmatrix} \sigma_x \\ \sigma_y \\ \tau_{xy} \end{Bmatrix}_k = \begin{bmatrix} \overline{Q}_{11} & \overline{Q}_{12} & \overline{Q}_{16} \\ \overline{Q}_{12} & \overline{Q}_{22} & \overline{Q}_{26} \\ \overline{Q}_{16} & \overline{Q}_{26} & \overline{Q}_{66} \end{bmatrix}_k \begin{Bmatrix} \varepsilon_x - \alpha_x \Delta T \\ \varepsilon_y - \alpha_y \Delta T \\ \gamma_{xy} - \alpha_{xy} \Delta T \end{Bmatrix}_k. \quad (19)$$

The equations in a contracted form can be written as

$$\sigma = \bar{Q}(\varepsilon - \alpha \Delta T), \quad (20)$$

where \bar{Q} is the plane stress stiffness tensor, α the thermal expansion coefficients tensors.

The general forces and moments corresponding the strains and curvatures of the thermo-elastic laminates by the classical relations is given

$$N = A\varepsilon + B\kappa - N_{\Delta T}; \quad (21)$$

$$M = B\varepsilon + D\kappa - M_{\Delta T}, \quad (22)$$

where, N and M are the tensors of in-plane forces and bending moments, ε is the strain tensor, κ the tensor of curvatures. $N_{\Delta T}$ and $M_{\Delta T}$ are the thermal stress and moments resultants, respectively. The A , B and D matrix is the elastic behavior in extension, coupling and bending, respectively. The above matrices are given by the following relations [32, 33]:

$$A = \sum_{k=1}^N \bar{Q}_k (z_k - z_{k-1}); \quad B = \frac{1}{2} \sum_{k=1}^N \bar{Q}_k (z_k^2 - z_{k-1}^2);$$

$$D = \frac{1}{3} \sum_{k=1}^N \bar{Q}_k (z_k^3 - z_{k-1}^3); \quad (23)$$

$$N_{\Delta T} = \sum_{k=1}^N \bar{Q}_k (\varepsilon_{\Delta T})_k (z_k - z_{k-1});$$

$$M_{\Delta T} = \frac{1}{2} \sum_{k=1}^N \bar{Q}_k (\varepsilon_{\Delta T})_k (z_k^2 - z_{k-1}^2). \quad (24)$$

3. NUMERICAL EXAMPLES

According to the Eq. 10 – Eq. 15, the material properties of every section point through-thickness are a function of thickness-direction coordinate z . The material properties of the upper surface (10% fiber fraction) and bottom surface (30% fiber fraction) can be determined, as shown in the Table 1.

The two different combination types of the two-layer [0°/90°] unsymmetric FGM shell is investigated: 1) the GF fraction along the thickness z direction change from lower to higher then to lower (L:H:L type), as shown in Fig. 1 a; 2) the GF fraction along the z direction change from higher to lower then to higher (H:L:H type), as shown in Fig. 1 b.

Table 1. Material properties of unidirectional composite components

	Young's Modulus, E , GPa	Poisson's ratio, μ	CTE, α , K^{-1}	Volume fraction, V
Glass Fibers (f)	27.84	0.22	5.0×10^{-6}	0.1~0.3
PP Matrix (m)	1.4	0.34	90.5×10^{-6}	0.9~0.7

ABAQUS software and its conventional shell element S4R are chosen to mesh the FGM laminated composites. Simpson's rule is adopted for integration method. Nine section points through the thickness of each layer and the

material properties of each section integration points are specified. Using the USDFLD subroutine, the corresponding functionally graded material properties can be attached to different section integration points. This computational model is a geometric nonlinear problem, the convergence depends on some control parameters. The central point of the shell is constrained as the displacement boundary condition.

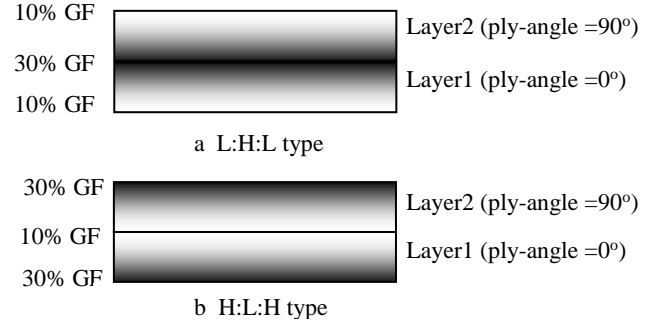


Fig. 1. Two Types of Un-symmetric FGM shell

The geometry parameters of the FGM flat plates at the initial state are: length $L = 151$ mm, width $B = 149$ mm, and vertical direction layer thickness $t_1 = t_2 = 0.255$ mm. The model is meshed into 900 shell elements and 961 nodes by type S4R shell element. The mechanical properties of the upper and bottom surface of one layer are shown in Table 2. Assuming volume fraction linear variation along the thickness direction, the corresponding mechanical properties of every section point can get by the Eq. 11 – Eq. 16. The central node in the model is restrained in all six degrees of freedom as the displacement boundary conditions.

Table 2. Material properties of the upper and bottom surface of one layer

	E_1 , GPa	E_2 , GPa	μ_{12}	G_{12} , GPa	α_1 , 10e-6/K	α_2 , 10e-6/K
10%	4.04	1.55	0.34	0.58	34.40	82.35
30%	9.33	1.96	0.33	0.73	17.56	66.05

3. 1. Two layer un-symmetric lay-ups

3. 1. 1. L:H:L type

In order to predict the equilibrium shapes, the procedure of the cool-down of the un-symmetric flat plates is from high temperature to room temperature. The FGM structure may change to a stable state in the first step which subjected to the whole temperature field variation. Here, the first stable state is reached when the temperature change from 180 °C to 20 °C, as shown in Fig. 2 b. Then the temperature gradient field of constant surface temperatures is imposed at the top and bottom surfaces. The variation of temperature is assumed to occur in the thickness direction only. Then when the temperature gradient is $\Delta T = 51$ °C, the model shape change to another shape after snap-through at the second step, as shown in Fig. 2 c. When the temperature gradient is removed and the initial room temperature field is reached, it is finally be the second stable state at the third load step, as shown in Fig. 2 d.

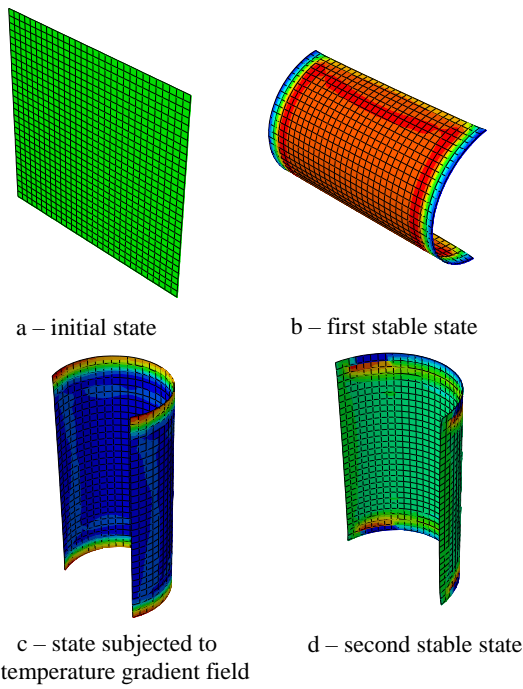


Fig. 2. Contour plot of the deformations and the von stresses distribution

3. 1. 2. H:L:H type

H:L:H type FGM shell also cool-down from 180 °C to 20 °C, then after applied the temperature gradient $\Delta T = 48.75$ °C, the second stable state is apparent. The structure shows different bi-stable properties because the different material component is varying along the thickness direction.

3. 2. Four layer anti-symmetric lay-ups

The more complex model, four layer anti-symmetric FGM shell, is studied in this part. The schematic representations of the FGM shell both L:H:L type and H:L:H type are shown in Fig. 3. Four anti-symmetric layers, such as $[0^\circ/90^\circ]_2$ and $[90^\circ/0^\circ]_2$ combination model, have discussed here. The geometry parameters of the FGM flat plates at the initial state are: length $L = 151$ mm, width $B = 149$ mm, and vertical direction layer thickness $t_1 = t_2 = t_3 = t_4 = 0.175$ mm. The model is also meshed into 900 shell elements and 961 nodes by type S4R shell element.

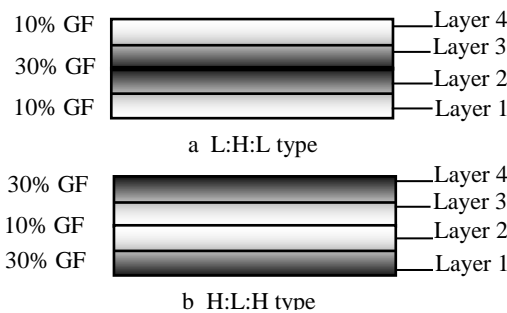


Fig. 3. Two types of anti-symmetric FGM shell

3. 2. 1. L:H:L type

The L:H:L type four-layer FGM composites including both $[0^\circ/90^\circ]_2$ and $[90^\circ/0^\circ]_2$ have the bi-stable

characteristics by the finite element simulation: 1) through the cool-down from 180 °C to 20 °C, the first stable can get, as shown in Fig. 4 first stable state; 2) the second stable state can get if the temperature gradient $\Delta T = 139.3$ °C to both two model, as shown in Fig. 4 second stable state.

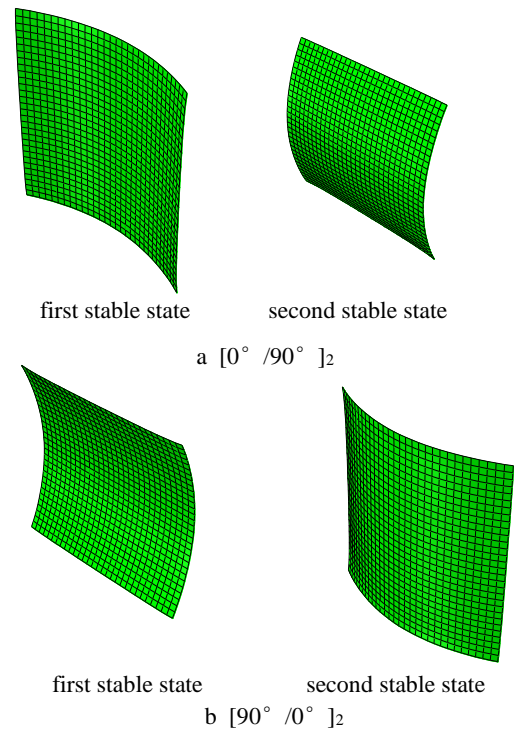


Fig. 4. Two stable states for the L:H:L type anti-symmetric FGM laminates

3. 2. 1. H:L:H type

The H:L:H type four-layer FGM composites including both $[0^\circ/90^\circ]_2$ and $[90^\circ/0^\circ]_2$ also considered. Through the cool-down from 180 °C to 20 °C, the first stable state of the $[0^\circ/90^\circ]_2$ and $[90^\circ/0^\circ]_2$ FGM shell can get, as shown in Fig.5 first stable state. Then, the second stable state can get if the temperature gradient $\Delta T = 70$ °C on opposite direction is applied to the $[0^\circ/90^\circ]_2$ and $[90^\circ/0^\circ]_2$ model, respectively, as shown in Fig. 5 second stable state. Both Fig. 4 and Fig. 5 show that there is different curvature direction and curvature radii for different kind of numerical examples.

Table 3. Two stables' curvature radii of the un-symmetric and anti-symmetric FGM composites

Lay-ups	FGM type	r_f , m	r_s , m
$[0^\circ/90^\circ]$	L:H:L	0.050	0.048
$[0^\circ/90^\circ]$	H:L:H	0.076	0.076
$[0^\circ/90^\circ]_2$	L:H:L	0.154	0.142
$[90^\circ/0^\circ]_2$	L:H:L	0.155	0.141
$[0^\circ/90^\circ]_2$	H:L:H	0.458	0.461
$[90^\circ/0^\circ]_2$	H:L:H	0.466	0.462

Table 3 gives the curvature radii of the first stable and second stable states, r_f and r_s , respectively. The table shows that the bi-stable characteristics are strongly influenced by different lay-ups, fiber direction, material properties and layer numbers. If we can predict the bi-stable behaviour

before producing, it is possible to manufacture bi-stable FGM composites which mechanical properties fit our needs.

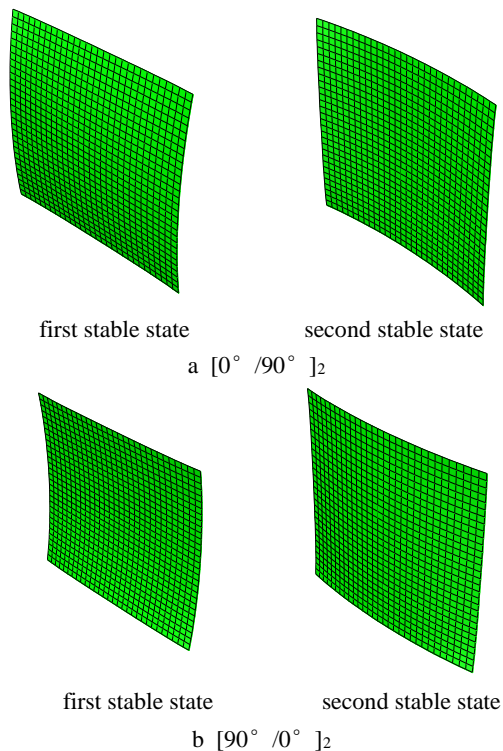


Fig. 5. Two stable states for the H:L:H type anti-symmetric FGM laminate

4. CONCLUSIONS

The bi-stability of the FGM shell subjected to a temperature gradient field is discussed. At the second stable state, the residual stress fields are retained in the structure. The bi-stable characteristics influenced by the fiber direction, the material properties, especially the thermal expansion coefficient for temperature field control the bi-stable problems, the lay-ups and the layer number. The paper presented a methodology to predict and control the equilibrium configurations of this kind laminates. Different un-symmetric and anti-symmetric orthogonal lay-ups numerical examples are discussed to show successful load path that brings the structure from one stable configuration to the other one.

Acknowledgments

This research was supported by the National Natural Science Foundation of China (Grant No. 51205355, 11372280), the Zhejiang Provincial Natural Science Foundation of China (Grant No. LY15E050016), the Research Fund for the Doctoral Program of Higher Education of China (Grant No. 20123317120003), the Postdoctoral Science Foundation of China (Grant No. 2013M540498).

REFERENCES

1. Gloria, A., Ronca, D., Russo, T., D'Amora, U., Chierchia, M., Santis, R. De Nicolais, L., Ambrosio, L. Technical Features and Criteria in Designing Fiber-

reinforced Composite Materials: from the Aerospace and Aeronautical Field to Biomedical Applications *Journal of Applied Biomaterials & Biomechanics* 9 2011: pp. 151–163.

2. Seferis, J.C., Nicolais, L. The Role of the Polymeric Matrix in the Processing and Structural Properties of Composite Materials, New York, Plenum, 1983. <http://dx.doi.org/10.1007/978-1-4615-9293-8>
3. Diaconu, C.G., Weaver, P.M., Mattioni, F. Concepts for Morphing Airfoil Sections Using Bi-stable Laminated Composite Structures *Thin-Walled Structures* 46 2008: pp. 689–701.
4. Iqbal, K., Pellegrino, S., Daton-Lovett, A. Bi-stable Composite Slit Tubes. Proc. IUTAM-IASS Symposium on Deployable Structures, Cambridge, 1998.
5. Iqbal, K., Pellegrino, S. Bi-stable Composite Shells *Proceedings of the 41st AIAA/ASME/ASCE/AHS/ASC Structures, Structural Dynamics, and Materials Conference and Exhibit* 2000: pp. 1–8.
6. Hyer, M.W. Calculations for the Room-temperature Shapes of Unsymmetric Laminates *Journal of Composite Materials* 15 1981: pp. 296–310.
7. Hyer, M.-W. The Room-temperature Shapes of Four-layer Unsymmetric Cross-ply Laminates *Journal of Composite Materials* 16 1982: pp. 318–340.
8. Dano, M.L., Hyer, M.W. SMA-induced Snap-through of Unsymmetric Fiber-reinforced Composite Laminates *International Journal of Solids and Structures* 40 2003: pp. 5949–5972.
9. Schultz, M.R., Hyer, M.W. Snap-through of Unsymmetric Cross-ply Laminates using Piezoceramic Actuators *Journal of Intelligent Material System and Structures* 14 2003: pp. 795–814. <http://dx.doi.org/10.1177/104538903039261>
10. Keadze, E., Guest, S.D., Pellegrino, S. Bistable Prestressed Shell Structures *International Journal of Solids and Structures* 41 2004: pp. 2801–2820. <http://dx.doi.org/10.1016/j.ijsolstr.2004.01.028>
11. Mattioni, F., Weaver, P., Potter, K., Friswell, M.I. Multi-stable Composites Application Concept for Morphing Aircraft, 16th International Conference on 'Adaptive Structures and Technologies', ICAST, 2005.
12. Tawfik, S., Tan, X., Ozbay, S., Armanios, E. Anticlastic Stability Modeling for Cross-ply Composites *Journal of Composite Materials* 41 2007: pp. 1325–1338.
13. Daynes, S., Potter, K.D., Weaver, P.M. Bistable Prestressed Buckled Laminates *Composites Science and Technology* 68 2008: pp. 3431–3437. <http://dx.doi.org/10.1016/j.compscitech.2008.09.036>
14. Galletly, D.A., Guest, S.D. Bistable Composite Slit Tubes. I. a Beam Model *International Journal of Solids and Structures* 41 2004: pp. 4517–4533.
15. Galletly, D.A., Guest, S.D. Bistable Composite Slit Tubes. II. a Shell Model *International Journal of Solids and Structures* 41 2004: pp. 4503–4516.
16. Guest, S.D., Pellegrino, S. Analytical Models for Bistable Cylindrical Shells *Proceedings of the Royal Society of London A: Mathematical, Physical and Engineering Sciences* 462 2006: pp. 839–854.
17. Portela, P., Camanho, P., Weaver, P.M., Bond, I. Analysis of Morphing, Multi-stable Structures Actuated by Piezoelectric Patches *Computers & Structures* 86 2008: pp. 347–356.

18. **Dano, M.L., Hyer, M.W.** Thermally-induced Deformation Behavior of Unsymmetric Laminates *International Journal of Solids and Structures* 35 1998: pp. 2101–2120.
[http://dx.doi.org/10.1016/S0020-7683\(97\)00167-4](http://dx.doi.org/10.1016/S0020-7683(97)00167-4)
19. **Dano, M.L., Hyer, M.W.** Snap-through of Unsymmetric Fiber Reinforced Composite Laminates *International Journal of Solids and Structures* 39 2002: pp. 175–198.
20. **Suresh, S., Mortensen, A.,** Fundamentals of Functionally Graded Materials, Processing and Thermomechanical Behaviour of Graded Metals and Metal-Ceramic Composites, the University Press, Cambridge, UK, 1998.
21. **Liew, K.M., He, X.Q., Ng, T.Y., Kitipornchai, S.** Active Control of FGM Plates Subjected to a Temperature Gradient: Modelling via Finite Element Method Based on FSDT *International Journal for Numerical Methods in Engineering* 52 2001: pp. 1253–1271.
<http://dx.doi.org/10.1002/nme.252>
22. **Li, L., He, X.Q., Zhu, H.P., Kitipornchai, S.** Bistable Characteristic of Laminated Shells with Graded Fibers *International Journal of Mechanics and Materials in Design* 7 2011: pp. 219–229.
<http://dx.doi.org/10.1007/s10999-011-9160-8>
23. **Jones, R.M.** Mechanics of Composite Materials, Second edition; PA, Taylor & Francis, 1999.
24. **Bolotina, K.S.** Coefficients of Thermal Expansion of Unidirectional Glass-reinforced Plastics *Mechanics of Composite Materials* 4 1968: pp. 568–570.
25. **Ishikawa, T., Koyama, K., Kobayashi, S.** Thermal Expansion Coefficients of Unidirectional Composites *Journal of Composite Materials* 12 1978: pp. 153–168.
26. **Kia, H.G.** Thermal Expansion of Sheet Molding Compound Materials *Journal of Composite Materials* 42 2008: pp. 681–695.
27. **Wetherhold, R.C., Seelman, S., Wang, J.** The Use of Functionally Graded Materials to Eliminate or Control Thermal Deformation *Composites Science and Technology* 56 1996: pp. 1099–1104.
28. **Jang, J., Lee, C.** Fabrication and Mechanical Properties of Glass Fibre-carbon Fibre Polypropylene Functionally Gradient Materials *Journal of Materials Science* 33 1998: pp. 5445–5450.
29. **Lee, N., Jang, J.** The Effect of Fibre-content Gradient on the Mechanical Properties of Glass-fibre-mat/polypropylene Composites *Composites Science and Technology* 60 2000: pp. 209–217.
[http://dx.doi.org/10.1016/S0266-3538\(99\)00122-0](http://dx.doi.org/10.1016/S0266-3538(99)00122-0)
30. **Vannucci, P., Verchery, G.** Stiffness Design of Laminates Using the Polar Method *International Journal of Solids and Structures* 38 2001: pp. 9281–9294.
[http://dx.doi.org/10.1016/S0020-7683\(01\)00177-9](http://dx.doi.org/10.1016/S0020-7683(01)00177-9)
31. **Vannucci, P., Vincenti, A.** The Design of Laminates with Given Thermal/hygral Expansion Coefficients, a General Approach Based upon the Polar-genetic Method *Composite Structures* 79 2007: pp. 454–466.
32. **Zhang, Z., Wu, H.L., He, X.Q., Wu, H.P., Bao, Y.M., Chai, G.-Z.** The Bistable Behaviors of Carbon-fiber/epoxy Anti-Symmetric Composite Shells *Composite Part B: Engineering* 47 2013: pp. 190–199.
<http://dx.doi.org/10.1016/j.compositesb.2012.10.040>
33. **Zhang, Z., Wu, H.P., Ye, G.F., Wu, H.L., He, X.Q., Chai, G.Z.** Systematic Experimental and Numerical Study of Bistable Snap Processes for Anti-Symmetric Cylindrical Shells *Composite Structures* 112 2014: pp. 368–377.